Article

Alloyed ZnCdS Nanocrystals with Highly Narrow Luminescence Spectral Width

Xinhua Zhong, Yaoyu Feng, Wolfgang Knoll, and Mingyong Han

J. Am. Chem. Soc., **2003**, 125 (44), 13559-13563• DOI: 10.1021/ja036683a • Publication Date (Web): 09 October 2003

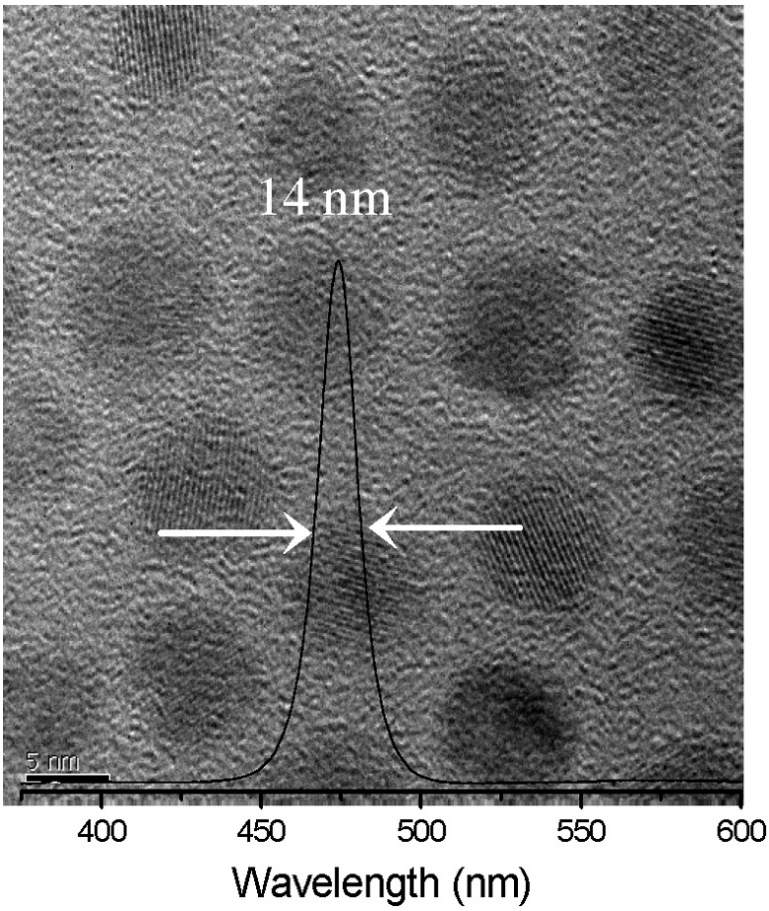

More About This Article

Additional resources and features associated with this article are available within the HTML version:

- Supporting Information

J|A|C|S
ARTICLES
Published on Web 10/09/2003

Alloyed $Zn_xCd_{1-x}S$ Nanocrystals with Highly Narrow Luminescence Spectral Width

Xinhua Zhong,[†] Yaoyu Feng,[§] Wolfgang Knoll,*[,†] and Mingyong Han*[,†,‡]

Contribution from the Department of Materials Science and Chemistry and the Department of Civil Engineering, National University of Singapore, Singapore 117543, and Institute of Materials Research and Engineering, 3 Research Link, Singapore 117602

Received June 14, 2003; E-mail: mashanmy@nus.edu.sg

Abstract: High-quality alloyed $Zn_xCd_{1-x}S$ nanocrystals have been synthesized at high temperature by the reaction of a mixture of CdO- and ZnO-oleic acid complexes with sulfur in the noncoordinating solvent octadecene system. A series of monodisperse wurtzite $Zn_xCd_{1-x}S$ ($x = 0.10, 0.25, 0.36, 0.53$) nanocrystals were obtained with corresponding particle radii of 4.0, 3.2, 2.9, and 2.4 nm, respectively. With the increase of the Zn content, their photoluminescence (PL) spectra blue-shift systematically across the visible spectrum from 474 to 391 nm, indicating the formation of the alloyed nanocrystals. The alloy structure is also supported by the characteristic X-ray diffraction (XRD) patterns of these nanoalloys with different Zn mole fractions, in which their diffraction peaks systematically shift to larger angles as the Zn content increases. The lattice parameter *c* measured from XRD patterns decreases linearly with the increase of Zn content. This trend is consistent with Vegard's law, which further confirms the formation of homogeneous nanoalloys. These monodisperse wurtzite $Zn_xCd_{1-x}S$ nanoalloys possess superior optical properties with PL quantum yields of 25−50%, especially the extremely narrow room-temperature emission spectral width (full width at half-maximum, fwhm) of 14−18 nm. The obtained narrow spectral width stems from the uniform size and shape distribution, the high composition homogeneity, and the relatively large particle radius, which is close to or somewhat larger than the exciton Bohr radius. The process by which the initial structure with random spatial composition fluctuations turns into an alloy (solid solution) with homogeneous composition is clearly demonstrated by the temporal evolution of the PL spectra during the annealing progress.

Introduction

Colloidal semiconductor nanocrystals (quantum dots, QDs) have generated great fundamental and technical interest due to novel size-tunable properties[1−5] and, consequently, in potential applications as optoelectronic devices and biomedical tags.[6−12] Among a variety of semiconductor materials, the binary II−VI nanocrystals have been most intensively investigated.[13−19] In the last two decades, the main efforts have been focused on the preparation of different color-emitting binary or core−shell nanocrystals with different particle sizes.[1,3] However, the tuning of physical and chemical properties by changing the particle size could cause problems in many applications, in particular, if unstable small particles (less than ∼2 nm) are used. Recent advances have led to the exploration of tunable optical properties by changing their constituent stoichiometries in mixed ternary nanocrystals.[20−25] Zhong and co-workers reported ternary $Zn_xCd_{1-x}Se$ alloyed nanocrystals with luminescent properties comparable or even better than the best-reported binary CdSe-based nanocrystals.[26] A color-tunable emission of the alloyed $Zn_xCd_{1-x}Se$ nanocrystals can be achieved by changing the

[†] Department of Materials Science and Chemistry, National University of Singapore.
[§] Department of Civil Engineering, National University of Singapore.
[‡] Institute of Materials Research and Engineering.

(1) Henglein, A. *Chem. Rev.* **1989**, *89*, 1861.
(2) Bawendi, M. G.; Steigerwald, M. L.; Brus, L. E. *Annu. Rev. Phys. Chem.* **1990**, *41*, 477.
(3) Alivisatos, A. P. *Science* **1996**, *271*, 933.
(4) Heath, J. R., Ed.; *Acc. Chem. Res.* **1999**, 32, 389−414.
(5) Murray, C. B.; Kagan, C. R.; Bawendi, M. G. *Annu. Rev. Mater. Sci.* **2000**, *30*, 545.
(6) Colvin, V. L.; Schlamp, M. C.; Alivisatos, A. P. *Nature* **1994**, *370*, 354.
(7) Tessler, N.; Medvedev, V.; Kazes, M.; Kan, S. H.; Banin, U. *Science* **2002**, *295*, 1506.
(8) Klimov, V. I.; Mikhailovsky, A. A.; Xu, S.; Malko, A.; Hollingsworth, J. A.; Leatherdale, C. A.; Eisler, H. J.; Bawendi, M. G. *Science* **2000**, *290*, 314.
(9) Sun, S. H.; Murray, C. B.; Weller, D.; Folks, L.; Moser, A. *Science* **2000**, *287*, 1989.
(10) Bruchez, M.; Moronne, M.; Gin, P.; Weiss, S.; Alivisatos, A. P. *Science* **1998**, *281*, 2013.
(11) Chan, W. C. W.; Nie, S. M. *Science* **1998**, *281*, 2016.
(12) Han, M. Y.; Gao, X. H.; Su, J. Z.; Nie, S. M. *Nat. Biotechnol.* **2001**, *19*, 631.
(13) Murray, C. B.; Norris, D. J.; Bawendi, M. G. *J. Am. Chem. Soc.* **1993**, *115*, 8706.
(14) Hines, M. A.; Guyot-Sionnest, P. *J. Phys. Chem.* **1996**, *100*, 468.
(15) Peng, X.; Schlamp, M. C.; Kadavanich, A. V.; Alivisatos, A. P. *J. Am. Chem. Soc.* **1997**, *119*, 7019.
(16) Dabbousi, B. O.; Rodriguez-Viejo, J.; Mikulec, F. V.; Heine, J. R.; Mattoussi, H.; Ober, R.; Jensen, K. F.; Bawendi, M. G. *J. Phys. Chem. B* **1997**, *101*, 9463.
(17) Peng, Z. A.; Peng, X. *J. Am. Chem. Soc.* **2001**, *123*, 183.
(18) Qu, L.; Peng, X. *J. Am. Chem. Soc.* **2002**, *124*, 2049.
(19) Yu, W. W.; Peng, X. *Angew. Chem., Int. Ed.* **2002**, *41*, 2368.
(20) Harrison, M. T.; Kershaw, S. V.; Burt, M. G.; Eychmüller, A.; Weller, H.; Rogach, A. L. *Mater. Sci. Eng., B* **2000**, *69*, 355.
(21) Korgel, B. A.; Monbouquette, H. G. *Langmuir* **2000**, *16*, 3588.
(22) Wang, W.; Germanenko, I.; El-Shall, M. S. *Chem. Mater.* **2002**, *14*, 3028.
(23) Kulkarni, S. K.; Winkler, U.; Deshmukh, N.; Borse, P. H.; Fink, R.; Umbach, E. *Appl. Surf. Sci.* **2001**, **169**, 438.
(24) Petrov, D. V.; Santos, B. S.; Pereira, G. A. L.; Donegá, C. D. M. *J. Phys. Chem. B* **2002**, *106*, 5325.
(25) Bailey, R. E.; Nie, S. *J. Am. Chem. Soc.* **2003**, *125*, 7100.

10.1021/ja036683a CCC: $25.00

particle composition besides the particle size. In a continuing effort, we report here the synthesis of ternary wide band gap $Zn_xCd_{1-x}S$ nanocrystals with superior optical properties. In particular, we demonstrate the narrowest room-temperature emission spectral width (full width at half-maximum, fwhm) of 14 nm in an ensemble measurement, which is comparable to the homogeneous line width of single CdSe QDs at room temperature.[27−30] The obtained high-quality $Zn_xCd_{1-x}S$ nanocrystals will be very promising nanomaterials as biological labels and short wavelength optoelectronic devices such as quantum dot lasers, high-density optical recording devices, photovoltaic cells, and displays.

Experimental Section

Chemicals. Oleic acid (tech, 90%), octadecene (tech, 90%), ZnO (99.999%), and sulfur powder (99.98%) were purchased from Aldrich. CdO (99.999%) was purchased from Strem.

Synthesis of $Zn_xCd_{1-x}S$ Nanocrystals. Most of the details of the synthetic and characterization methods were similar to those reported in the literature.[17−19] For a typical preparation of $Zn_xCd_{1-x}S$, sample a ($x = 0.10$), a mixture of CdO (0.0064 g, 0.05 mmol), ZnO (0.0081 g, 0.10 mmol), oleic acid (0.5 mL), and octadecene (4.0 mL) were heated to ~80 °C and degassed under a vacuum of 10 Pa for 20 min. The reaction vessel was then filled with argon, and its temperature was increased to 310 °C. After the CdO and ZnO precursors were dissolved completely to form a clear colorless solution, the temperature was lowered to 300 °C. A solution of sulfur (1.0 mL, 0.0032 g, 0.10 mmol) in octadecene was swiftly injected into this hot solution within 1 s, and the reaction mixture was kept at 300 °C for the subsequent growth and annealing of the resulting nanocrystals. Aliquots of the sample were taken at different time intervals, and UV−vis and PL spectra were recorded for each aliquot. These sampling aliquots were quenched in cold chloroform (25 °C) to terminate growth of the particles immediately. For making different color-emitting nanocrystals, a series of $Zn_xCd_{1-x}S$ samples b, c, and d with different compositions were also prepared under the same conditions as sample a, except for the different amounts of ZnO and S used (0.15, 0.20, and 0.30 mmol for both ZnO and S, respectively).

Characterization. UV−vis and PL spectra have been obtained on a Shimadzu UV-1601 spectrometer and a RF-5301 PC fluorometer, respectively. Room-temperature PL efficiencies were determined by comparing the integrated emission of the QDs samples in chloroform with that of fluorescent dye, coumarin 540 with identical optical density. Excitation wavelengths were set at the first absorption peak of the QD samples. A quadratic refractive index correction was done when two different solvents were used to dissolve QDs and dyes.[31] Also, the known efficiencies of the QDs in solution can be used to measure the efficiencies of other QDs by comparing their integrated emission or PL intensity of solutions. Low concentration of solutions was used to avoid obvious reabsorption.

The resulting nanocrystals in chloroform solution were precipitated with methanol and further isolated by centrifugation and decantation. The excess amounts of both ligands and reaction precursors were removed by extensive purification prior to the measurements using high-resolution transmission electron microscopy (HRTEM), powder X-ray diffraction (XRD), and inductively coupled plasma atomic emission (ICP). All the measurements were performed on original QD samples without any size sorting. A JEOL JEM3010 transmission electron microscope (operated at an accelerating voltage of 300 kV) was used to analyze size, size distribution, and structure of the alloyed nanocrystals deposited on the Formvar-carbon-coated copper grids. The size distribution histograms for all the samples were obtained by analyzing more than 200 crystallites in each sample. The XRD patterns for the final products were recorded by a Siemens D5005 X-ray powder diffractometer. The compositions for the alloyed nanocrystals were measured by means of ICP using a standard HCl/HNO_3 digestion.

Results and Discussion

The high-resolution TEM images of the obtained $Zn_xCd_{1-x}S$ nanocrystals (Figure 1) reveal uniform spherical nanocrystals with well-resolved lattice fringes, demonstrating the highly crystalline nature of the nanocrystals. All the as-prepared $Zn_xCd_{1-x}S$ nanocrystals of (a) 4.0, (b) 3.2, (c) 2.9, and (d) 2.4 nm in radius with corresponding Zn mole fractions of 0.10, 0.25, 0.36, and 0.53, respectively, have narrow size distributions with a relative standard deviation of 5−8% without any size sorting (refer to the size distribution histograms of samples a−d in the Supporting Information). Powder XRD of the nanocrystals reveals a wurtzite hexagonal structure of the ternary alloyed nanocrystals over all compositions (Figure 2). The characteristic XRD patterns of the alloyed nanocrystals exhibit seven prominent peaks, which are indexed to the scattering from (100), (002), (101), (102), (110), (103), and (112) planes, respectively. Because of finite size-broadening effects, the XRD peak width of the alloyed nanocrystals in Figure 2 increases gradually with the decrease of particle size. The XRD peaks also shift to larger angles gradually as the Zn content increases. The continuous peak shifting of the nanocrystals may also rule out phase separation or separated nucleation of CdS or ZnS nanocrystals. As shown in Figure 3, the lattice parameter *c* measured from the XRD patterns of the $Zn_xCd_{1-x}S$ nanocrystals exhibits a nearly linear relationship with the Zn compositions. A gradual decrease in the lattice parameter *c* is observed as the Zn composition (*x*) increases. This trend is consistent with Vegard's law and indicates a homogeneous alloy structure.[32,33] Vegard's law was applied to check the compositional homogeneity in bulk and diluted magnetic semiconductor nanocrystals.[33−35]

The PL and absorption spectra of the $Zn_xCd_{1-x}S$ alloyed nanocrystals with different Zn mole fractions are shown in Figure 4. It is observed that the excitonic absorption peak gradually disappears with increasing particle size. For each $Cd_xZn_{1-x}Se$ sample, the peak emission wavelength is Stokes-shifted slightly to longer wavelength than that of the excitonic absorption peak, indicating that the band-edge emission dominates the PL of the alloyed QDs without the deep-trap emission at longer wavelengths, which is commonly encountered for binary CdS QDs. The obtained alloyed QDs exhibit extremely narrow spectral widths of 14−18 nm and high luminescent quantum yields of 25−50% on ensemble measurements at room temperature. Typical PL spectral widths of QDs are generally around 27−40 nm. Peng reported an ensemble of CdSe nanocrystals with fwhm of the PL peak as narrow as 23 nm.[17] To the best of our knowledge, the observed 14 nm spectral width

(26) Zhong, X. H.; Han, M. Y.; Dong, Z. L.; White, T. J.; Knoll, W. *J. Am. Chem. Soc*. **2003**, *125*, 8589.
(27) Li, X. Q.; Arakawa, Y. *Phys. Rev. B* **1999**, *60*, 1915.
(28) van Sark, W. G. J. H. M.; Fredrix, P. L. T. M.; Van den Heuvel, D. J.; Asselberg, M. A. H.; Gerritsen, H. C. *Single Mol*. **2000**, *1*, 291.
(29) Michalet, X.; Pinaud, F.; Lacoste, T. D.; Dahan, M.; Bruchez, M. P.; Alivisatos, A. P.; Weiss, S. *Single Mol*. **2001**, *4*, 261.
(30) van Sark, W. G. J. H. M.; Fredrix, P. L. T. M.; Van den Heuvel, D. J.; Gerritsen, H. C. *J. Phys. Chem. B* **2001**, *105*, 8281.
(31) Demas, J. N.; Crosby, G. A. *J. Phys. Chem*. **1971**, *75*, 991.
(32) Vegard, L.; Schjelderup, H. *Phys. Z*. **1917**, *18*, 93.
(33) Furdyna, J. K. *J. Appl. Phys*. **1988**, *64*, R29.
(34) Hanif, K. M.; Meulenberg, R. W.; Strouse, G. F. *J. Am. Chem. Soc*. **2002**, *124*, 11495.
(35) Jun, Y.-w.; Jung, Y.-y.; Cheon, J. *J. Am. Chem. Soc*. **2002**, *124*, 615.

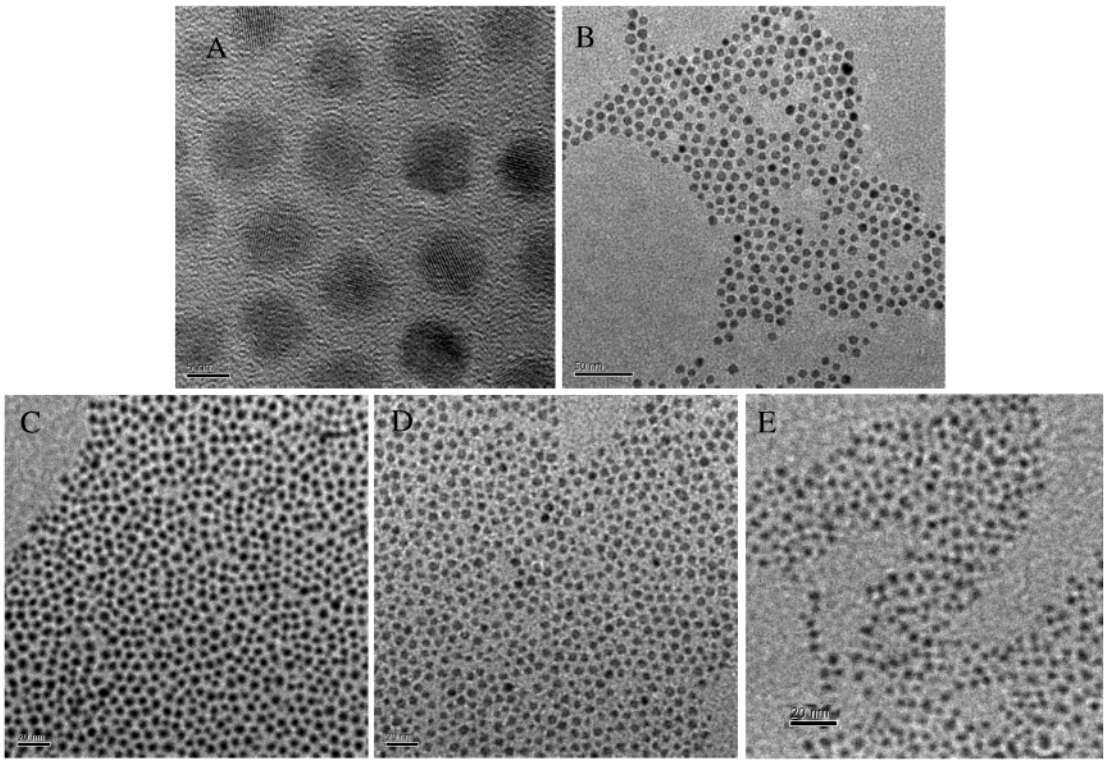

Figure 1. TEM images of the $Zn_xCd_{1-x}S$ nanocrystals: (A) HRTEM image of sample a, $Zn_{0.10}Cd_{0.90}S$; (B) TEM overview images of sample a, $Zn_{0.10}Cd_{0.90}S$; (C) sample b, $Zn_{0.25}Cd_{0.75}S$; (D) sample c, $Zn_{0.36}Cd_{0.64}S$; and (E) sample d, $Zn_{0.53}Cd_{0.47}S$.

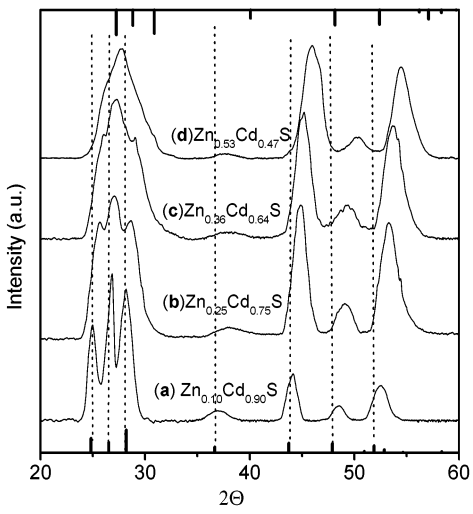

Figure 2. Powder XRD patterns of the $Zn_xCd_{1-x}S$ samples a−d. The line XRD spectra correspond to bulk hexagonal CdS (bottom) and bulk hexagonal ZnS (top), respectively.

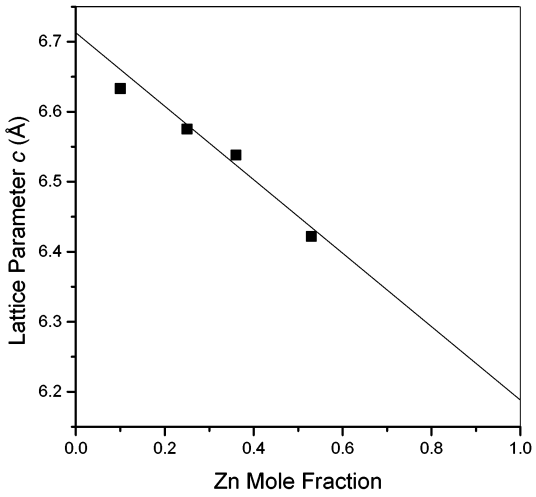

Figure 3. A linear relationship of the lattice parameter *c* of the $Zn_xCd_{1-x}S$ nanoalloys as a function of Zn mole fractions, which is measured from XRD patterns (square data points) and calculated from Vegard's law (solid line).

should be the narrowest one for QDs ensembles at room temperature. This spectral width is similar to the homogeneous line width observed in single dot spectroscopy by phonon-dephasing processes,[27−30] which eliminates the effect of inhomogeneous broadening due to size fluctuations at room temperature. It is clear that the inhomogeneous spectral broadening is effectively suppressed in these alloyed nanocrystals ensembles.

Semiconductor nanocrystals with a dot radius significantly smaller than the exciton Bohr radius show strong size-dependent optical properties due to the strong quantum confinement effect (QCE) of the charge carriers in all three dimensions. A weak quantum confinement effect occurs when the particle radius is close to or somewhat larger than the Bohr radius. For semiconductor nanocrystals, inhomogeneous broadening arises, first, from the finite size distribution.[36,37] It was known that in the weak QCE regime, where $R_{r/B}$ (ratio of particle radius and exciton Bohr radius) is larger than 1, the finite size distribution translates into a relatively small variation in the band gap energy and, consequently, a narrow emission spectral width instead of a significantly large variation in the strong QCE regime, where $R_{r/B}$ is far less than 1.[36,37] Typical exciton Bohr radii range from

(36) Gaponenko, S. V. *Optical Properties of Semiconductor Nanocrystals*; Cambridge University Press: Cambridge, 1998.
(37) Krishna, M. V. R.; Friesner, R. A. *J. Chem. Phys*. **1991**, *95*, 8309.

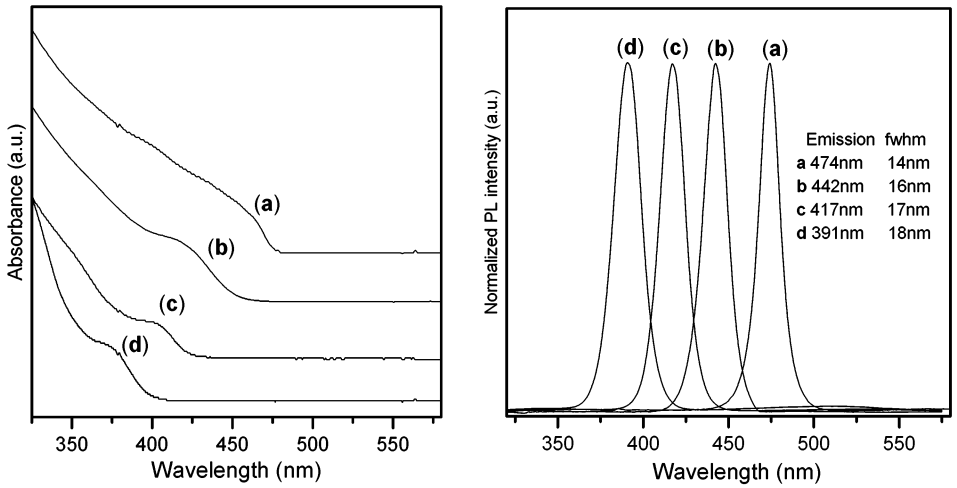

Figure 4. Ensemble UV−vis (left) and PL spectra (right, $\lambda_{ex} = 300$ nm) for the $Zn_xCd_{1-x}S$ samples a−d.

2.2 nm (ZnS), 3.0 nm (CdS), 5.6 nm (CdSe), to 7.5 nm (CdTe) in II−VI semiconductors. For similar size range, the QCE is more pronounced in materials with smaller band gap energy and larger Bohr radius (or less pronounced in materials with larger band gap energy and smaller Bohr radius).[36] The mostly investigated CdSe nanocrystals with particle radius close to or somewhat larger than the Bohr radius of 5.6 nm are not readily prepared. With the use of wide band gap ZnS and CdS with small Bohr radii, the high-quality ternary $Zn_xCd_{1-x}S$ nanocrystals of 2.4−4.0 nm in radius in the weak QCE regime have been successfully prepared, whereas this size range of CdSe still corresponds to the strong confinement regime. The obtained $Zn_xCd_{1-x}S$ nanocrystals are in the weak QCE regime because the particle sizes of 4.0, 3.2, 2.9, and 2.4 nm in radius are close to or larger than the corresponding Bohr radii of samples a−d (Bohr radii of (a) $Zn_{0.10}Cd_{0.90}S$, (b) $Zn_{0.25}Cd_{0.75}S$, (c) $Zn_{0.36}Cd_{0.64}S$, and (d) $Zn_{0.53}Cd_{0.47}S$ are 2.92, 2.80, 2.71, and 2.58 nm, respectively). Thus, inhomogeneous broadening due to size fluctuations is tremendously suppressed, which maybe the main reason for the extremely narrow spectral width of the alloyed nanocrystals. The fabrication of highly luminescent alloy nanocrystals with the radii around the corresponding Bohr radius bears the potential to significantly improve the performance of QD-based optoelectronic devices, which is mainly limited by the inhomogeneous broadening in the optical properties because of the size inhomogeneity.

The size effect on the band gap energies of the obtained alloyed QDs is further discussed here. It should be pointed out that the particle radii of samples a−d decrease from 4.0 to 2.4 nm monotonically. The particle radii of the obtained alloyed nanocrystals, which are close to or somewhat larger than the Bohr radius, correspond to the weak QCE regime. As reported by Weller et al., the band gap energy difference between CdS particles with the radii of 4.8 and 2.8 nm is very small (0.08 eV or 12 nm from 476 to 462 nm).[38] The decrease in particle radius (2 nm) has limited contribution to the increase of the band gap energy because of the weak QCE. As stated above, the relatively small decrease in particle radius (1.6 nm) from samples a−d cannot lead to an obvious variation in the band gap energy. Thus, the significant band gap energy increase from samples a−d (wavelength difference of 83 nm) mainly arises from the compositional variation instead of size effect. As shown in Figure 4, the excitonic absorption peaks disappear gradually as particle size increases. The largest $Zn_{0.10}Cd_{0.90}S$ nanocrystals (sample a) exhibit almost the same features of absorption spectra shape as bulk crystals (no observable excitonic absorption), indicating that the QCE is extremely weak. When the particle size is further approached to the corresponding Bohr radius, weak excitonic absorption peaks are observed as shown in the UV−vis spectra, which indicates the existence of a limited QCE but no obvious contribution to inhomogeneous spectral broadening as discussed above.

The most direct and immediate evidence for the alloying process can be probed from the continuous shift of the absorption and PL spectra of the obtained nanocrystals with different compositions. With the increase of the Zn mole fractions from 0.10 to 0.53, a systematic blue-shift was observed in Figure 4 for both the first excitonic absorption onsets and the band-edge emission peaks (from 474, 442, and 417 to 391 nm) of the resulting ternary nanocrystals. This significant blue-shift provides clear evidence for the formation of the alloyed $Zn_xCd_{1-x}S$ nanocrystals via intermixing the wider band gap ZnS (3.7 eV) with the narrower band gap CdS (2.5 eV), rather than forming separate CdS, ZnS, or core−shell-structured nanocrystals. If CdS or ZnS nucleates separately, the corresponding PL and absorption peaks of CdS and ZnS nanocrystals should appear. The sole PL and absorption peak of the resulting nanocrystals in our reaction system rule out the separate nucleation, which is in agreement with the results of TEM and XRD measurements. If a core−shell structure is formed, such a significant shift of the optical spectra cannot be produced compared with those of the core materials. The alloy structure is also proved by the finding that the identical emission wavelengths of the obtained $Zn_xCd_{1-x}S$ nanocrystals cannot be obtained by the binary CdS or ZnS nanocrystals with the same particle size as the $Zn_xCd_{1-x}S$ nanocrystals. The relationship between the Zn compositions and the peak emission wavelength of the alloyed nanocrystals is shown in Figure 5. The data of bulk alloy are also plotted against the Zn mole fraction for comparison.[39] A nearly linear relationship or a small bowing parameter is observed in the two systems. In addition, the

(38) Vossmeyer, T.; Katsikas, L.; Giersig, M.; Popvic, I. G.; Diesner, K.; Chemseddine, A.; Eychmuller, A.; Weller, H. *J. Phys. Chem.* **1994**, *98*, 7665.

(39) Hill, R. *J. Phys. C: Solid State Phys.* **1974**, *7*, 521.

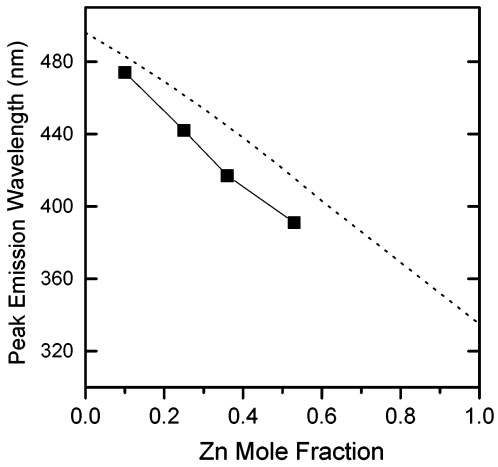

Figure 5. Dependence of the peak emission wavelength of the alloyed nanocrystals (solid line) and bulk $Zn_xCd_{1-x}S$ (dashed line) on their compositions.

experimental lattice parameter *c* is consistent with Vegard's law, indicating the homogeneous distribution of ZnS and CdS in the alloyed nanocrystals.

The question that naturally comes is why the obtained $Zn_xCd_{1-x}S$ composites are a homogeneous alloy (solid solution) rather than a structure with a concentration gradient. Our research results indicate that the growth rate of CdS is larger than that for ZnS in the investigated reaction system. Without considering atom diffusion, theoretically the CdS concentration should be higher in the interior than that in the exterior of the composite QDs and vice versa for ZnS, whereas the internal atom diffusion at the high-preparation temperature can convert the original structure with spatial composition fluctuations into a homogeneous alloy. This is clearly demonstrated in the previously reported alloyed $Zn_xCd_{1-x}Se$ system.[26]

As shown in Figure 6, this alloying process is clearly demonstrated by the temporal evolution of the PL spectra during the high-temperature annealing progress, where the initial broad, asymmetric band-edge PL peak (corresponding to a structure with random spatial composition fluctuations) gradually turns into a narrow and symmetric one (corresponding to the alloy structure with composition homogeneity). The component homogeneity, achieved through the internal atom diffusion at high temperature, may have a contribution to the narrow PL spectral width. Furthermore, the thermal annealing can eliminate the original deep-trap emission by removing the crystallite defects. This finding can also explain the wide spectral width (usually fwhm >50 nm) usually accompanied with the strong deep-trap emission for the previously reported composite QDs prepared at room temperature.[20−23] Because of the low preparation temperature, the internal atom diffusion is not efficient and thus results in an compositional inhomogeneity of the nanoparticle system, which may have a major contribution to the wide spectral width. It is also observed in Figure 6 that the quantum yield and PL profile (peak shape and position) of the alloyed $Zn_xCd_{1-x}S$ QDs can be fixed for 3 h. That is, the final emission wavelength is predetermined by the composition of the reactants, and the influence from the Oswald ripening can be neglected. These properties make this method a very reproducible and controllable method to obtain high-quality QDs with specified emission wavelengths.

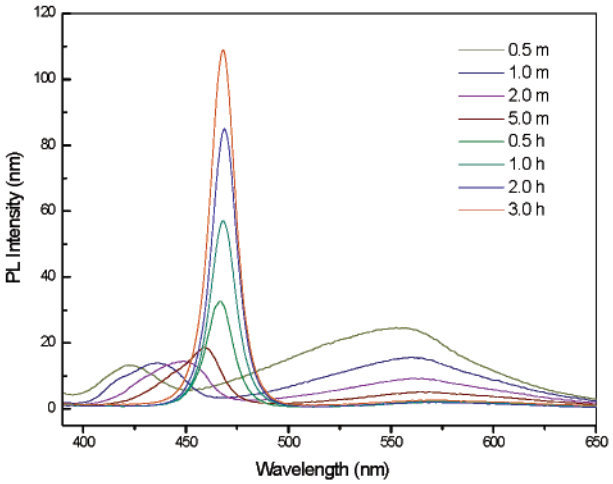

Figure 6. Temporal evolution of the PL spectra of $Zn_{0.10}Cd_{0.90}S$ nanocrystals (sample a) grown at 300 °C in a mixture of 0.5 mL of oleic acid, 0.05 mmol CdO, 0.10 mmol ZnO, and 4 mL of ODE.

In summary, we have successfully synthesized high-quality alloyed $Zn_xCd_{1-x}S$ nanocrystals with high luminescent quantum yields and extremely narrow emission spectral widths of 14−18 nm. This highly narrow spectral width mainly arises from the uniform particle size and shape, the high homogeneity in composition, and the relatively large $R_{r/B}$ corresponding to the weak QCE regime.

Acknowledgment. We gratefully acknowledge the Institute of Materials Research and Engineering and the National University of Singapore. Part of this material is also based upon work sponsored by the Science & Engineering Research Council of Singapore under Grant No. MCE/TP/00/001-2.

Supporting Information Available: Size distribution histograms for all the samples (PDF). This material is available free of charge via the Internet at http://pubs.acs.org.

JA036683A